Structure-activity-relationship studies to elucidate sources of antibacterial activity of modular polyacrylate microgels

Carlie M. Clem,‡ Babloo Sharma,‡ and Susanne Striegler*

Department of Chemistry and Biochemistry, 345 North Campus Drive, University of Arkansas, Fayetteville, Arkansas, 72701, United States.

KEYWORDS. Antibacterial, polyacrylate microgel, Staphylococcus aureus, synergistic effect, binuclear copper(II) complex

ABSTRACT: Emerging infections of unknown origin and increasing bacterial resistance against available antibiotics necessitate the development of different antimicrobial agents with unconventional mechanisms of action. A promising strategy to meet this need may be found by combining polymeric scaffolds with transition metals, e.g. by decorating polyacrylate-based microgels with Cu(II) complexes. A series of structure activity relationship studies using broth microdilution assays with such material and *Staphylococcus aureus* concluded that the antimicrobial activity of the microgels can be tailored during their synthesis by choice of comonomers; by design of the binding strength between Cu(II) ions and backbone ligands; and by selection of the counter ions for coordination to the metal complexes. A microgel ^{Cu} P(EG) (L = VBbsdpo) with an optimized minimal inhibitory concentration of 0.39 ± 0.03 µg/mL is thereby derived and synthesized from 60 mol% of crosslinking ethyleneglycol dimethacrylate, 40 mol% butyl acrylate, 0.5 mol% VBbsdpo ligand with 1 mol% Cu(II) ions, and 5 mol% ethylene glycol as counter ions. The antimicrobial activity of the microgel has a lifetime of over 18 months at ambient temperature. Bactericidal activity of the same microgel is observed by re-plating assays in less than 15 min when exposing *S. aureus* to microgel concentrations of 1.5-fold of its MIC value or higher. Furthermore, spectrophotometric evaluations at 260 nm revealed time- and concentration-dependent release of intracellular bacterial components after interactions with the microgel indicating irreversible damage to the bacterial cell membrane as a possible mechanism of activity. Preliminary results indicate that the selected microgels are not cytotoxic toward human dermal fibroblasts at MIC value concentrations for over 20 h.

Introduction.

The looming futility of current antibiotic treatments demands a timely development of new therapeutic agents to combat the increasing threat of drug-resistant microbes.^[1] In efforts to develop effective strategies, polymeric scaffolds, such as gels, [2; 3] micelles, [4] nanomaterials, [5] as well as metalbased nanoparticles^[6] have emerged showing promising preliminary results as antimicrobial agents. Along these lines, polymeric scaffolds are used to carry known low molecular weight antibiotics^[4; 7] and to transport antimicrobial peptides whose primary mechanism of action is to disrupt bacterial membranes. [3; 8; 9] Additionally, polymers have been designed to possess intrinsic antimicrobial activity due to a strong cationic character that adversely interacts with anionic components of bacterial surfaces leading to membrane disruption. [10; ^{11]} Metal nanoparticles can likewise damage bacterial membranes via electrostatic interactions and disrupt biological processes by releasing metal ions or by generating reactive oxygen species.[6; 12]

Another promising, yet largely untapped, resource toward the development of new antibacterial agents is the use of metal complexes. [13; 14] Coordination compounds offer unique mechanisms of action, charges, and a broad range of geometries, which may be beneficial in addressing currently known bacterial resistance mechanisms. [13] Numerous examples show an-

timicrobial activity of transition metal coordination complexes and bio-organometallic derivatives that are typically higher for the metal-containing coordination compound than for the free ligands. [15-17] However, many complexes show limited potential as antimicrobial agents due to insufficient water-solubility or inadequate stability in aqueous solution. Notable efforts to circumvent these inherent problems are made by functionalization of the ligand backbones of the metal complexes with water solubility-promoting functional groups or by mounting on peptide strains.^[18] In other efforts to obtain strong antimicrobial agents, metal ions such as Ni(II) and Cu(II) ions are coordinated to already known antibiotic sulfonamides and found to increase the apparent antimicrobial activity overall. [19; However, as the activity of many complexes remains outside of the susceptibility range toward bacteria (MIC \leq 32 or 16 μg/mL) at unknown cytotoxicity, metal complexes are often precluded from further consideration as effective antimicrobial agents. Nevertheless, a recent systematic screening of metal complexes from a 960-member library disclosed 88 complexes in the susceptibility range of selected Grampositive and Gram-negative bacteria. [13] Among the active and not toxic complexes, inorganic coordination compounds derived from Pt, Ag, Pd, Ir, and Cu are frequently observed. [13]

Combining both emerging strategies by immobilizing metal complexes onto polymeric support thus appears a very attractive and promising strategy with the potential to enable new treatment options toward multi-drug resistant bacteria in the long term. In a recent proof-of-concept study, we demonstrated the antimicrobial activity of microgels with embedded copper(II) complex and showed a 4-fold better performance of the microgels over commercially available vancomycin. [21] Briefly, the selected *Staphylococcus aureus* strain is susceptible to a series of polyacrylate microgels whose activity is linked to the degree of crosslinking. Intermediate activity or resistance was observed for interactions between the bacteria and selected low molecular weight antibiotics under comparable conditions. [21]

The microgel body is typically composed of ethyleneglycol dimethacrylate (1, EGDMA) crosslinker, butyl acrylate (BA) monomer, and a metal coordinating ligand such as pentadentate VBbpdpo (2) (Chart 1). [4; 21] Then, copper(II) acetate is added to a pre-polymerization mixture to transform the ligand in-situ into copper(II) complexes, followed by addition of excess of coordinating counter ions, such as mannose, to prevent the copper(II) ions from interfering with the radical polymerization. [22-24] Ultra-sheering of the monomer mixture in an aqueous buffer-surfactant system yields in the presence of stabilizing hydrophobes defined droplets which are captured as particles by free-radical polymerization under UV light. [25; 26] The resulting microgels are spherical particles with pre-defined hydrodynamic diameters between 150 and 280 nm (Figure 1). [21; 27] An optimal antimicrobial activity was observed for microgels with a crosslinking content of 60 mol%.[21]

To propose a possible mode of action and obtain preliminary data for the interaction between *S. aureus* and the microgels, the contributions of the structural components of the microgel architecture toward the apparent antimicrobial activity are determined in a systematic structure-activity-relationship study. The shelf-life of the microgel activity is examined, and time- and concentration-dependent bactericidal properties of the material highlighted. Additionally, time- and concentration-dependent membrane damage is observed by the release of absorbing intracellular components. Finally, preliminary data are obtained to characterize the cytotoxicity of the microgels towards human dermal fibroblasts.

Results and Discussion

With a library of microgels on hand^[24; 27-29] that are prepared in presence of different counter ions, with altered matrix compositions, and selected immobilized metal complexes, their antimicrobial activity toward *S. aureus* was evaluated.^[21; 30] The structure-activity study using broth microdilution assays is a first step toward elucidating the mechanism of action. The results of this study allow streamlining of the modular material syntheses to essential building blocks, and highlight the contributions of each component toward the overall activity.

Influence of counter ions on the antimicrobial activity of the resulting microgels

For an initial set of experiments, all microgels contain 60 mol% of ethyleneglycol dimethacrylate crosslinker, 40 mol% of butyl acrylate (BA) monomer, and 0.5 mol% of the

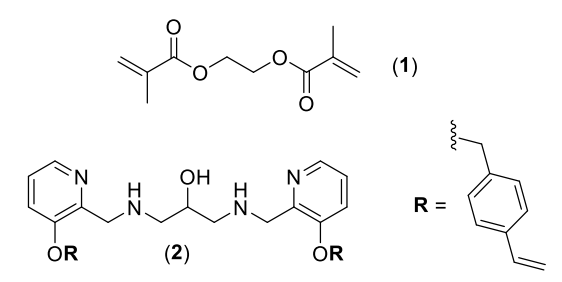


Chart 1. Structures of EGDMA (1) and VBbpdpo (2)

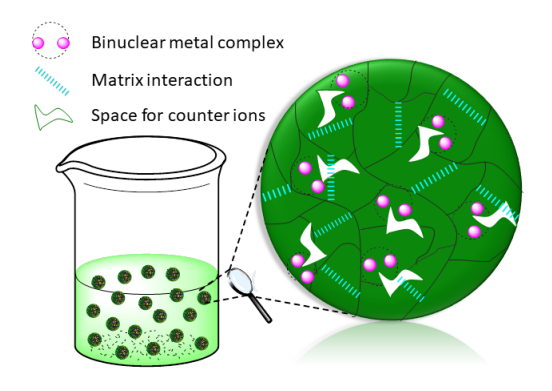


Figure 1. Typical structure of a microgel

Chart 2. Structures of counter ions used during material synthesis.

Table 1. Minimum inhibitory concentration of microgels ${}^{\text{Cu LP}}_{2}\text{P}_{60\%}$ against *S aureus* (ATCC® 25923TM)

Entry	Anion	$MIC [\mu g/mL]$	
1	amidine (3)	0.52 ± 0.02	
2	Man (4)	0.64 ± 0.01	
3	EG (5)	0.73 ± 0.02	
4	Gal (6)	0.75 ± 0.03	
5	TEG (7)	1.06 ± 0.03	

VBbpdpo ligand coordinated to copper(II) ions. Following the previously developed synthetic strategy, [24] a diverse selection of counter anions (**Chart 2**) was employed to determine the resulting structure-activity relationship and streamline future microgel syntheses.

The antimicrobial activity of the resulting gels is highest when N-4-methylbenzyl-D-galactonoamidine (3, amidine) or mannose (4)^[23] are used to chelate the metal core during syn-

thesis (**Table 1, Entries 1-2**). [23; 31] The activity decreases when ethylene glycol (**5**, EG), [27] galactose (**6**) [27] and triethylene glycol (**7**, TEG) are employed (**Table 1, Entries 3-5**). The binding of compounds **3-7** as counter anions to the immobilized binuclear Cu(II) centers decreases in the same order. This observation indicates a correlation between the metal binding strength of the anion during synthesis and the antimicrobial activity of the resulting material favoring strong metal complex coordination.

Influence of the matrix composition on the antimicrobial activity of the resulting microgels

For the second set of experiments, all microgels contain 1.75 mmol of polymerizable monomer. While the crosslinking content was kept constant at 60 mol %, 20 mol% of the monomer are BA, and 20 mol% are one of the selected comonomer acrylates (8)a-h (Chart 3, Table 2). As before, all microgels contain 0.5 mol% of the ligand VBbpdpo that was immobilized in presence of Cu(II) acetate and excess mannose (4). Due to the nature of the experiments, the microgel ${}^{\text{Cu}}_{2}{}^{\text{L}}P_{60\%}$ prepared in presence of mannose in the first set of experiments (Table 1, entry 2) and the microgel with 20 mol% of BA in the second set of experiments (Table 2, entry 4) are identical. Interestingly, all microgels prepared in presence of polar comonomers 4-hydroxyethyl acrylate (8a), 2-methoxyethyl acrylate (8b) and 2-hydroxyethyl acrylate (8c) (Table 2, entries 1-3) show higher antimicrobial activity than the benchmark microgel synthesized from butyl acrylate (8d). All other comonomers 8e-h (Table 2, entries 5-8) are less polar than 8d, and the corresponding microgels show a lower antimicrobial activity. The polarity of the monomers 8b-h was estimated from their dipole moment in a computational approach previously, [29] the dipole moment for 8a is added in this study (see Supporting Information). Overall, the polarity of the monomers decreases in the given order from 8a to 8h and thus parallels the observed antimicrobial activity. For optimization of the microgel performance, the use of commercially available polar co-monomer acrylate appears preferable over the use of a costly amidine (3) (Table 1, entry 1) and gives comparable results. The experiments document the influence of H-bond donating and accepting building blocks in the polymer matrix on the overall observed antimicrobial activity of the material and show higher antimicrobial activity for microgels prepared from a selection of polar building blocks.

Influence of the ligand structure and complex stability on the antimicrobial activity of the resulting microgels

In a third set of experiments, the microgel synthesis is evaluated by alteration of the immobilized metal complexes. While a recent study documented the contributions of the immobilized Cu₂VBbpdpo complex on the antimicrobial activity of the corresponding microgels, [21] the ligand preparation is quite tedious and time-consuming. Premature polymerization during solvent removal, and chromatographic purification often leads to diminished yields or even complete compound loss, and impure batches of ligand. Additionally, the shelf-life of the obtained ligand oil is short (5-7 days) even under inert atmosphere, in the dark at -18 °C. Identification of suitable functional ligands promoting comparable antimicrobial activity while

Chart 3. Structures of acrylate co-monomers 8a-h

Table 2. Minimum inhibitory concentration of microgels ${}^{\text{Cu L}}_{2}\text{P}_{60\%}$ (acrylate) against *S. aureus*, L = VBbpdpo

Entry	Co-monomer (8)	MIC [μg/mL]
1	8a	0.50 ± 0.03
2	8b	0.51 ± 0.01
3	8c	0.53 ± 0.01
4	8d	0.64 ± 0.01
5	8e	0.66 ± 0.01
6	8f	0.68 ± 0.01
7	8g	0.70 ± 0.03
8	8h	0.72 ± 0.01

Chart 4. Structures of VBbsdpo (9) and VB(IDA) (10)

exhibiting increased shelf-life stability and ease of handling is thus desirable.

Therefore, microgels are synthesized using pentadentate ligand VBbsdpo (9) and bidentate VB(IDA) (10) in addition to VBbpdpo (2) (Chart 4). The corresponding Cu(II) complexes are binuclear for complexes derived from 9^[22] and mononuclear for complexes derived from 10.^[32] All microgels are synthesized in presence of 60 mol% of EGDMA and 40 mol% BA, copper(II) acetate, and excess of mannose following the described protocols.^[24] The amount of immobilized ligands was determined by gravimetric analyses from the degree of polymerization during microgel synthesis at 60 min as described.^[24] The amount of formed Cu(II) complexes is quantitative and determined under rebinding conditions by isothermal calorimetric titrations.^[22; 33] Broth microdilution assays

reveal lower minimum inhibitory concentration for microgels with immobilized Cu(II) complexes derived from VBbsdpo (9) and VBIDA (10) than for VBbpdpo (2) (Table 3). The results indicate a strong influence of the immobilized metal complex on the antimicrobial activity of the material and identify $^{\text{Cu}}_{2}{}^{9}P_{60\%}$ as the microgel with the highest antimicrobial activity among those evaluated (Table 3, Entry 1). The minimal bactericidal activity for this microgel is as low as 0.5 $\mu\text{g/mL}$.

To rationalize the observations, we estimated the amount of free Cu(II) ions leaking from the immobilized complexes using the known binding constants of the respective nonpolymerizable low molecular weight Cu(II) complexes. [22; 32] The calculation estimates 13 ng/mL of free Cu(II) ions leaking from Cu_2bpdpo (11) $(pK_a = 17)$, [22; 34] and 6 ng/mL each leaking from $Cu_2TEGbsdpo$ (12) $(pK_a = 30)$, [22] and CuIDA (13) $(pK_a = 11)^{[32]}$ under the given experimental conditions (Chart 5). While free Cu(II) ions show a MIC value above 500 µg/mL and are thus not the source of antimicrobial activity, [21] the amount of free metal ions nevertheless diminishes the apparent concentration of the immobilized complexes. Given that the molar amounts of immobilized ligand is identical for all polymers for all complexes while the molar amounts of free Cu(II) ions is not, the concentration of apparent Cu(II) complexes in the microgels increases from Cu₂2 over Cu₁₀ to Cu₂9. The observations imply a correlation between the apparent antimicrobial activity of the gels and the strength of the formation constant of the immobilized metal complex, while free Cu(II) ions themselves have no quantifiable contribution.

Lifetime of microgel activity

To evaluate the shelf-life stability of the microgels, aliquots of aging microgel dispersions are taken in regular time intervals and analyzed for alterations in their antibacterial activity. Four microgels $^{\text{Cu}_2}_{\ 2}^{\ L}P_{60\%}$, L = VBbsdpo (9) and VBbpdpo (2), using ethylene glycol and mannose as counter ions are selected from the library as representative examples of the most active microgels. Broth microdilution assays show that the antimicrobial activity of all microgels is maintained over more than 18 months (see Supporting Information).

This finding is in sharp contrast to the storage requirements of other antimicrobial agents. For example, vancomycincontaining ophthalmic solutions with 0.005 % benzalkonium chloride as preservative are reported to maintain their potency for 60 days when stored at ambient temperature and for 6 months when frozen at -10 and -25 °C. [35] Vancomycin hydrochloride stabilized with 5% dextrose solution maintains 90% of its potency for at least 58 days when stored at 4 °C in polyvinyl chloride bags despite discoloring and strongly altered pH of the solution. [36] Similarly prepared vancomycin solutions maintain their antimicrobial activity over 28 days, but drop to only 40 or 55% of initial activity at 60 days, when stored at 5 or 25 °C. [37] As a consequence, the developed antimicrobial microgels may offer an alternative to traditional agents when storage in the cold or repetitive renewing of supplies is limited or impossible. The results also disclose that

Table 3. Minimum inhibitory concentration of microgels with immobilized Cu(II) complex against *S. aureus*

Entry	L	MIC [μg/mL]	MBC [μg/mL]
1	9	0.39 ± 0.03	0.5
2	10	0.56 ± 0.02	1
3	2	0.64 ± 0.01	1

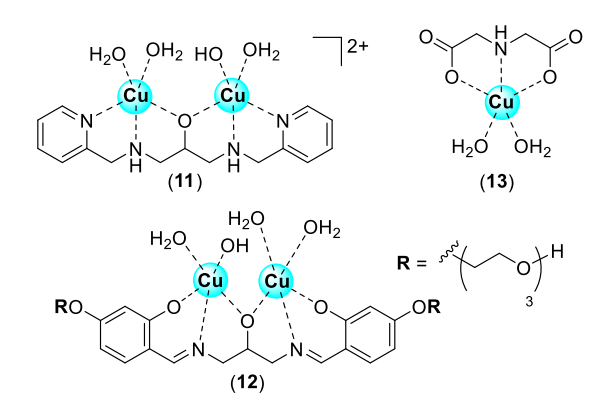


Chart 5. Non-polymerizable Cu(II) complex analogues

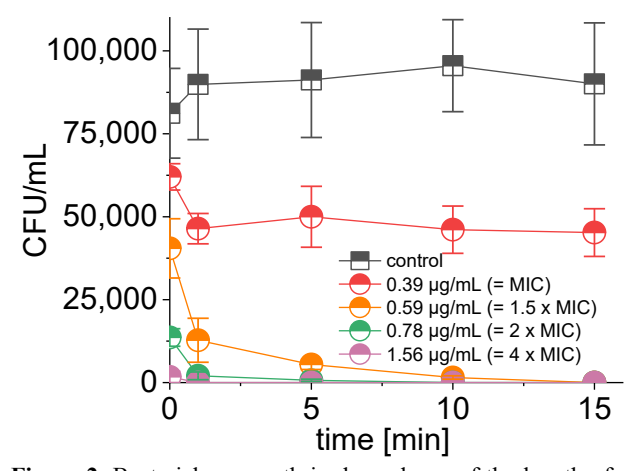


Figure 2. Bacterial re-growth in dependence of the length of exposure time and concentration of microgel $^{\text{Cu}}_{2}{}^{9}P_{60\%}$ (EG) after incubation at 37 °C for 24 h

polymers derived from ligand VBbsdpo (9) belong to the best performing microgels independent of the counter ion used during material synthesis (compare MIC of $^{\text{Cu}}_{2}{}^{9}P_{60\%}(EG) = 0.39 \pm 0.03~\mu\text{g/mL};$ and Entry 1, Table 3). The thermal and chemical stability of the microgels was already described. $^{\text{[24]}}$

Time-kill assays

Subsequently, the time to impact or extinct the re-growth of *S. aureus* was determined in dependence of the microgel concentration using $^{\text{Cu}}_{2}^{\text{L}}P_{60\%}(\text{EG})$ (L = VBbsdpo (9)) as a representative example. In a typical set of experiments, microgel dispersions are prepared so that their concentrations match the minimum inhibitory concentration or multiples thereof when exposed to equal volumes of bacterial suspensions. After in-

cubation of the combined microgel-bacteria suspensions for defined time intervals, aliquots are removed, diluted with saline solutions, and plated on Mueller Hinton agar. To assess the residual bacterial viability, images of the plates are taken after 24 h of incubation, and analyzed for bacterial re-growth by colony count.

Exposing $^{\text{Cu}}_{2}^{9}\text{P}_{60\%}(\text{EG})$ to *S. aureus* at its minimal inhibitory concentration results in a slight decrease of bacterial viability. The effect is more pronounced when using the microgel in concentrations that are multiples of its MIC value (**Figure 2**). In fact, the bacterial cell viability is zero in less than one minute when using the microgel at a concentration of 1.56 $\mu\text{g/mL}$ (4 × MIC); in less than 5 min for a microgel concentration of 0.78 $\mu\text{g/mL}$ (2 × MIC); and in about 15 min when using the microgel at 0.59 $\mu\text{g/mL}$ (1.5 × MIC). The results highlight the impressive antimicrobial activity of the microgel and the short required contact time to eliminate the re-growth ability of *S. aureus*.

260nm release study

After documenting the time requirements to kill bacteria upon contact with microgels, further insights toward a possible mode of action became desirable. As the diameters of the microgels are between 150 and 280 nm, their entry into *S. aureus* cells of 1 µm is rather unlikely. However, the bacterial cell membrane may be compromised or disrupted upon interaction with the microgels as reported for antimicrobial peptides. [38] Intracellular components, such as nucleotides, absorb light at 260 nm, and allow convenient quantification by UV/Vis spectroscopy. A release of intracellular compounds over 15% indicates irreversible damage of the bacterial cell membrane. [39]

Therefore, and as a first step toward elucidating the mechanism of action, different concentrations of Cu P P60% (EG) are exposed to S. aureus suspensions, and the release of absorbing bacterial cell compounds followed spectrophotometrically. In a typical experiment, the 260 nm absorbance of filtrates of bacterial suspensions is determined after exposure to ^{Cu}₂ P_{60%}(EG) over a 1 h interval (**Figure 3**). The microgel is chosen as a representative example and used in concentrations representing its MIC and MBC values, and multiples thereof. When using the microgel at its MIC value, bacteriostatic effects are observed. The release of bacterial cell components is below the 15 % threshold indicating a compromised cell membrane, that is, however, reversible. This interpretation agrees well with the re-growth behavior observed for the use of $^{\text{Cu}}_{2}{}^{9}\text{P}_{60\%}(\text{EG})$ at its MIC value during the time-kill studies discussed above. However, using the microgel in higher concentrations results in a fast release of intracellular bacterial components until an apparent maximal change of 24 % is reached in only 15 min. The corresponding irreversible damage of the bacterial membrane aligns well with the fast killing kinetics observed in the solution-based time-kill study at comparable concentrations.

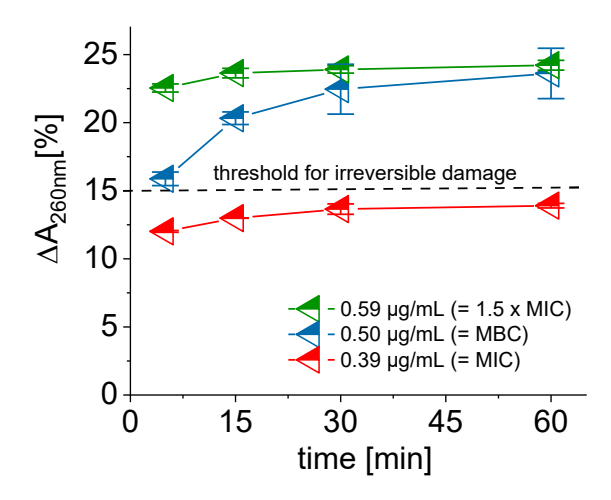


Figure 3. Time-dependent change of absorbance at 260 nm for filtrates of S. aureus suspensions exposed to microgel $^{\text{Cu}}_{2}{}^{9}P_{60\%}(\text{EG})$

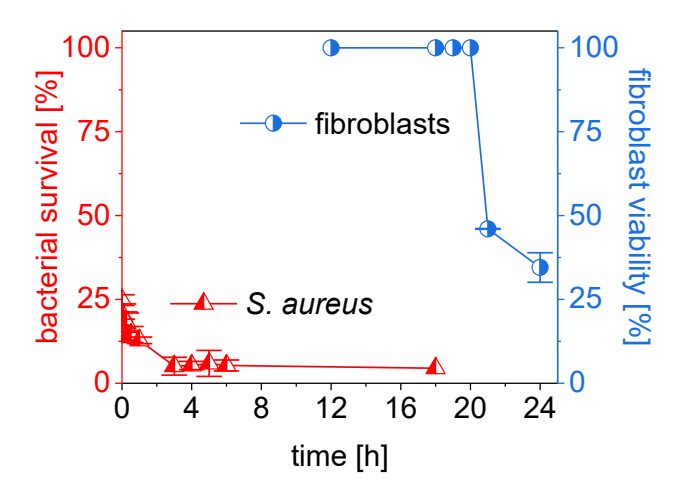


Figure 4. Time-dependent survival of bacteria and fibroblasts upon exposure to $^{\text{Cu}}_{2}{}^{9}P_{60\%}(EG)$ at 0.39 µg/mL (MIC value)

Cytotoxicity

As the developed microgels show strong bactericidal activity, they may also show toxicity toward human cells. Therefore, we grew human dermal fibroblasts from seed cells at 37 °C in a humid 5% CO₂ atmosphere. When the growth medium is changed every 2-3 days, the confluence of the cells reaches 80-90 % in about 10-12 days.

In a typical 96-well plate assay, the fibroblasts are used non-attached in a concentration of 10^5 cells/mL and incubated with $^{\text{Cu}}_{2}{}^{9}P_{60\%}(\text{EG})$ at 0.39 µg/mL (MIC value) and control compounds at corresponding concentrations for up to 24h. The assay is read out after addition of resazurin dye and extended incubation by recording of fluorescence intensities ($\lambda_{\text{ex}} = 535 \text{nm}$, $\lambda_{\text{em}} = 595 \text{nm}$). [40] Metabolically active cells will thereby reduce the non-fluorescent blue dye to fluorescent pink resorufin. [41] Cells without any antimicrobial additive are treated likewise and used as controls. The recorded fluorescence intensities are given as an average of eight independent cell dispersions and corrected for background effects. The residual

cell viability is calculated from the deduced data as a percent value relative to untreated cells.^[42]

The viability of the fibroblasts is unaffected by the treatment with $^{\text{Cu}}_{2}^{9}P_{60\%}(\text{EG})$ for at least 20 h, after which the cell viability sharply declines to 46% at 21 h and 35% at 24 h (**Figure 4**). The viability of the fibroblasts remains unaffected and larger than 99% for SDS/CAPS buffer, Cu(II) acetate, Cu₂bpdpo, EGDMA crosslinker, and the BA monomer controls for more than 21 h. The observation indicates apparent cytotoxicity of the microgel itself after 20 h. However, the proof-of-concept study emphasizes the viability of the fibroblast over extended time, while the bacterial regrowth ability drops to about 5% after exposure to identical concentrations of $^{\text{Cu}}_{2}^{9}P_{60\%}(\text{EG})$. The combined observations indicate a strong potential of the microgel as an antimicrobial agent on surfaces with a low risk for humans upon contact.

Conclusions

The study obtained preliminary data to characterize the interactions between S. aureus and polyacrylate microgels and highlights the synergy of matrix and metal complex contributions toward the overall antimicrobial activity of the material. Initially, a systematic structure-activity study disclosed in three steps contributions of the structural components of the microgel architecture toward their apparent antimicrobial activity: (i) strongly coordinating counter ions used during material preparation ensure optimized antimicrobial activity of the resulting material; (ii) the choice of polar monomers reduces the MIC values of the resulting material, and allows the use of commercially available counter ions in place of galactonoamidine that has to be synthesized in 16 steps; and (iii) the immobilized metal complex has the strongest effect on the overall antimicrobial activity of the microgel independent of the counter ions used during material preparation, i.e. microgels prepared from ligand VBbsdpo show generally higher antimicrobial activity than comparable microgels synthesized from VBbpdpo or VBIDA. The antimicrobial activity increases parallel to the binding strength of the respective Cu(II) complexes from Cu₂bpdpo to CuIDA and Cu₂bsdpo. The results allow streamlining of the modular microgel syntheses to focus on essential building blocks. Broth microdilution assays of aliquots of aging microgel solutions highlight a shelf-life of the microgel activity of over 18 months. Exposing bacteria suspensions to equal volumes of ${}^{Cu}_{2}^{L}P_{60\%}(EG)$ (L = VBbsdpo (9)) at concentrations resembling its MIC value or multiples thereof show bactericidal activity of the microgel in re-plating experiments in less than 15 min when the concentration is 1.5 times of the MIC value or higher.

Evidence for interactions between bacteria and microgel at the bacterial cell membrane is obtained by quantification of the absorbing intracellular components using UV/Vis spectroscopy at 260 nm. At the MIC value of the microgels reversible permeation of the bacterial membrane is observed, while higher concentrations lead to irreversible damage. Additionally, viability assays of the selected microgel with human dermal fibroblasts reveal that the material is not cytotoxic for 20 h. The combined results of the study allow streamlining of

the modular microgel synthesis to essential components and provide the foundation for a potential use of the gels as antimicrobial agents on surfaces.

Experimental details

Instrumentation.

For fibroblast growth, a Heracell VIOS 160i CO₂ incubator (Thermo Scientific), a NU-407FM-400 biosafety cabinet (NuAire), a Heraeus Multifuge X3R centrifuge (Thermo Scientific), an Eclipse E200 microscope (Nikon), an inverted CP-2A1 Inverted Compound Microscope (Jenco), and a Thermo Scientific LP Vortex Mixer were used. The instrumentation used for the growth of *S. aureus*, and for the synthesis and characterization of microgels was described. UV spectra and fluorescence intensities were obtained on a F5 Filtermax multimode microplate reader (Molecular Devices); the bacterial cell suspensions were matched to McFarland standards using a Cary50 UV/Vis spectrophotometer (Varian) with temperature-controlled multi-cell changer.

Materials and methods.

General remarks.

Protocols for the synthesis of microgels,^[24] procedures for the computational assessment of the dipole moment of **8a**,^[29] a protocol for the growth of *S. aureus*, broth microdilution assays, and the procedure for determination of minimal bactericidal concentration are described and used as such.^[21]

Polystyrene tissue culture flasks treated for increased cell attachment (VWR International) were used for fibroblast growth; disposable hemocytometers with Neubauer Improved grid and 0.1 mm depth (INCYTO) for manual cell count; clear medium-binding, flat-bottom, chimney 96-well black polystyrene microplates with clear lids (Greiner Bio-One); heatresistant polyester films (VWR) for fibroblast viability; clear medium-binding, flat-bottom, chimney 96-well microlon ELISA plates for determination of minimal inhibitory concentrations and time-kill studies; Acrodisc sterile syringe filters with a 0.2 μm Supor Membrane (Pall Laboratory) for separating 260 nm absorbing material from *S. aureus* suspensions; disposable polycyclical olefin 1.5 mL semi-micro cells with 10 mm path length (BrandTech) for measuring UV/VIS data.

The ligands *N*, *N'*-1,3-bis[(2-hydroxy-4-vinylbenzyloxy)benzylideneamino]propan-2-ol, VBbsdpo (9)^[22] and vinylbenzyliminodiacetic acid, VBIDA (10),^[32] are synthesized as described. The microgels ^{Cu}₂ ^LP_{60%} are synthesized in presence of counter anions *N*-4-methylbenzyl galactonoamidine (3),^[28] mannose (4),^[27] ethylene glycol (5 EG),^[24] and galactose (6),^[24]; from acrylate co-monomers 8b-h;^[29] and with binuclear Cu(II) complex derived from *N*, *N'*-1,3-bis((3-(4-vinylbenzyloxy)pyridin-2-yl)methylamino)propan-2-ol, VBbpdpo (2), as communicated.^[27] Bacterial cell forming unites are counted using the naked eye or ImageJ, v1.53a, image processing software.

Chemicals, bacteria, and mammalian cells

All chemicals for microgel synthesis were obtained from commercial suppliers at reagent grade or higher and used as received if not noted otherwise. Triethylene glycol (7) was obtained from Sigma-Aldrich; 4-hydroxybutyl acrylate (8a) from TCI America; and ethanol from Koptec. All acrylates were filtered over neutral alumina immediately prior to use.

Fetal bovine serum was obtained from VWR International; antibiotic-antimycotic solution containing 10,000 units of penicillin, 10 mg streptomycin, and 25 μg amphotericin B per mL from MP Biomedicals; Trypan blue solution from GE Healthcare Life Sciences; resazurin dye from BioLegend; and phosphate buffered saline solution from VWR Life Science; *Staphylococcus aureus* (ATCC® 25923TM), human dermal fibroblasts CCD-986Sk (ATCC® CRL-1947TM), Iscove's modified Dulbecco's medium and trypsin-EDTA solution were obtained from the American Type Culture Collection.

Microgel synthesis and characterization

General procedure for the preparation of a monomer pre-polymerization mixture

In a typical experiment, a pre-polymerization mixture was prepared from an 0.4012 g (1.75 mmol) aliquot containing 0.2081 g (1.049 mmol, 60 mol%) of EGDMA, and 0.090 g (0.7022 mmol, 40 mol%) of BA in 9.6 g aqueous 52 mM SDS/50 mM CAPS solution, 0.0817 g of decane, an aliquot of the selected ligand stock solution, a 100 μl aliquot of an 177 mM aqueous copper(II) acetate solution, and a 250 μL aliquot of a 355 mM aqueous stock solution of the selected counter anion. The pre-polymerization mixture is sonicated by ultrasheering, and polymerized in the cold as described. $^{[24]}$

Microgel Cu₂²P_{60%}(TEG)

A 90.9 mg aliquot of VBbpdpo (2) in DMSO is added from ligand stock solution (0.1063 g of 2 in 2.1034 g of solution in DMSO), and triethylene glycol (7) is used as a counter ion; the ligand concentration in the microgel is 578 μ g/ml (1.077 mM); Anal. calcd for C, 62.28; H, 7.81; N, 0.16; found: C, 61.27; H, 7.66; N, 0.20; $D_h = 240 \pm 4$ nm.

Microgel Cu 9P60%.(Man)

A 115.51 mg aliquot of VBbsdpo (9) in DMSO is added from the ligand stock solution (34.56 mg of 2 in 808.57 mg of solution in DMSO), and mannose (4) is used as a counter ion; the polymerization progress is 66% at 60 min with a ligand concentration of 312 μ g/ml (0.555 mM) in the microgel; Anal. calcd for C, 62.30; H, 7.81; N, 0.08; found: C, 61.10; H, 7.16; N, 0.0; $D_b = 267 \pm 4$ nm.

Microgel Cu 9P60% (EG)

A 115.51 mg aliquot of VBbsdpo (9) in DMSO is used from the ligand stock solution (34.56 mg of 2 in 808.57 mg of solution in DMSO), and ethylene glycol (5) as a counter ion; the polymerization progress is 57% at 60 min with a ligand concentration of 272 μ g/ml (0.484 mM) in the microgel; Anal. calcd for C, 62.30; H, 7.81; N, 0.08; found: C, 60.97; H, 7.30; N, 0.10; $D_b = 204 \pm 4$ nm.

Microgel Cu10 P60% (Man)

A 109.03 mg aliquot of VBIDA (10) in DMSO is used from the ligand stock solution (17.56 mg of 2 in 763.23 mg of solution in DMSO), and mannose (4) as a counter ion; the polymerization progress is 84.5 % at 60 min with a ligand concentration of 203 μ g/ml (0.713 mM) in the microgel; Anal. calcd for C, 62.04; H, 7.82; N, 0.04; found: C, 60.98; H, 7.39; N, 0.00; D_h = 259 \pm 2 nm.

Microgel Cu10P60%(EG)

A 109.03 mg aliquot of VBIDA (10) in DMSO is used from the ligand stock solution (17.56 mg of 2 in 763.23 mg of solution in DMSO), and ethylene glycol (5) as a counter ion; the polymerization progress is 75 % at 60 min with a ligand concentration of 183 μ g/ml (0.640 mM) in the microgel; Anal. calcd for C, 62.04; H, 7.82; N, 0.04; found: C, 61.77; H, 7.42; N, 0.00; $D_h = 223 \pm 4$ nm.

Microgel Cu₂P_{60%, 8a}(Man)

The monomer pre-polymerization mixture containing 1.75 mmol monomer made of 60 mol% EGDMA, 20 mol% BA and 20 mol% **8a** was prepared from an 0.3048 g aliquot of a monomer mixture containing 0.2084 g (1.051 mmol) of EGDMA, 0.045 g (0.3511 mmol) of BA and 0.0510 g (0.3540 mmol) of **8a**; a 0.1163 g aliquot of VBbpdpo (**2**) in DMSO (68.42 mg in 1678 mg of solution in DMSO) in 9.6 g 52 mM SDS/50 mM CAPS solution; a 100 μ l aliquot of an 177 mM aqueous copper(II) acetate solution; a 250 μ L aliquot of a 355 mM aqueous mannose (**4**) solution and 0.0812 g of decane; the ligand concentration is 407 μ g/ml (0.757 mM); Anal. calcd for C, 61.15; H, 7.68; N, 0.16; found: C, 60.37; H, 7.60; N, 0.15; D_h = 145 ± 3 nm.

General procedure for the treatment of microgels prior to exposure to bacterial or mammalian cells

The synthesized microgel dispersions are purified prior to use by successive dialyses against aqueous sodium ethylenediamine tetraacetate/ sodium dodecylsulfate and *N*-cyclohexyl-3-aminopropanesulfonic acid/ sodium dodecylsulfate solutions as described.^[21] The resulting dispersions are treated with appropriate volumes of aqueous Cu(II) acetate solution, diluted 5-fold with aqueous CAPS/SDS solution, and stored at ambient temperature until use. The ligand concentration of the resulting microgels dispersions is typically 64-90 µg/mL.

Assays with bacteria

Bacterial growth

S. aureus was grown as described;^[21] the absorbance of an aliquot of the cell suspension was adjusted to the absorbance of a 0.5 McFarland standard to estimate the concentration of the resulting cell suspension as 1×10^8 CFU/mL.

Lifetime of microgel activity

Previously described broth microdilution assays for the determination of minimal inhibitory concentrations^[21] are used here to determine the time-dependent residual activity of microgel dispersions stored at ambient temperature.

For 96-well plate assays, aliquots of a freshly prepared S. aureus suspension are diluted with Mueller-Hinton broth and

used as stock solutions with a nominal concentration of 5 \times 10^5 CFU/mL. Aliquots of aging dispersions of $^{\text{Cu}}_{2}{}^{2}P_{60\%}(\text{EG})$, $^{\text{Cu}}_{2}{}^{2}P_{60\%}(\text{Man})$, $^{\text{Cu}}_{2}{}^{9}P_{60\%}(\text{EG})$ and $^{\text{Cu}}_{2}{}^{9}P_{60\%}(\text{Man})$ with a concentration of 64 µg/mL are taken after 1, 118, 297, and 550 days (\approx 18 months), and incubated with *S. aureus* at 37°C. The apparent minimal inhibitory concentration of the microgels is determined from absorbance reads at 595 nm as described. $^{[21]}$ The lifetime of the microgel activity is obtained from the comparison of the residual activity after storage to the minimal inhibitory activity at day 1.

Time-kill assays

General remarks. For the time-kill assays, aliquots of a freshly prepared S. aureus suspension are diluted with Mueller-Hinton broth and used as stock solutions with a nominal concentration of 5×10^5 CFU/mL. Additionally, Mueller-Hinton broth is used to prepare dispersions of $^{\text{Cu}}_{2}{}^{9}P_{60\%}(\text{EG})$ with a nominal ligand concentration of 0.78, 1.18, 1.56, and 3.12 μ g/mL. All microgels dispersions are steam-sterilized and stored at ambient temperature until use.

Assay preparation. In a typical experiment, 100 μ L of $^{^{\text{Cu}}_{^{9}}\text{P}}_{60\%}(EG)$ microgel dispersions are incubated with 100 μ L of bacterial suspensions in sealed medium-binding, flatbottom 96-well plates at 37 °C and shaking at 240 rpm. The nominal bacterial cell count in this assay is 2.5×10^5 CFU/mL, the resulting microgel concentrations are 0.39, 0.59, 0.78, and 1.56 μ g/mL. After selected points in time, 40 μ L aliquots are removed from the ongoing incubation and diluted with 2000 μ L of 0.9 % sterile saline solution. Then, 50 μ L aliquots of the diluted samples are plated on Mueller Hinton agar and incubated at 37 °C for 24 h. For control experiments, equal volumes of broth instead of microgels are added to the bacteria and treated likewise. All experiments are performed with a minimum of three independently grown bacterial suspensions.

Data analysis. After incubation, all plates are imaged and the apparent bacterial colonies are counted by naked eye or by using ImageJ software. The number of cell forming units is then correlated to the volume of the plated aliquot and the sample dilution prior to plating. The deduced residual concentration of bacteria is given as an average of three experiments and graphed over time.

Mechanistic studies - 260 nm release studies

General remarks. For mechanistic studies, a 125 μ L aliquot of the adjusted *S. aureus* suspension is diluted with sterile 0.9 wt % saline solution to 25 mL and used as a stock solution with a nominal bacterial concentration of 5 × 10⁵ CFU/mL. Additionally, dispersions of $^{\text{Cu}}_{2}{}^{9}P_{60\%}(\text{EG})$ in saline solution are prepared with a nominal ligand concentration of 0.78, 1.00, and 1.18 μ g/mL. All microgels dispersions are steam-sterilized and stored at ambient temperature until use.

Assay preparation. Equal volumes of *S. aureus* and microgel stock solutions are mixed and incubated at 37 °C under gentle shaking at 240 rpm for 5, 15, 30 and 60 min. Subsequently, the absorbance of the filtrate is recorded at 260 nm. For control experiments, microgel dispersions are substituted by equal amounts of saline solution. All experiments are conducted in triplicate.

Data analysis. For each time point, the absorbance reads of filtrates obtained from bacterial suspensions with microgel are averaged and expressed as percent relative to absorbance reads of filtrates of microgel-free bacterial suspensions. The change in absorbance is plotted over time.

Mechanistic studies - cytotoxicity

Growth of human dermal fibroblasts

Growth initiation. The purchased fibroblasts were thawed, transferred to complete growth medium comprised of Iscove's modified Dulbecco's medium supplemented with 10 % (v/v) fetal bovine serum and 1 % (v/v) antibiotic-antimycotic solution, and seeded initially in a 25 cm² tissue culture flask at a density of 1×10^4 cells/ cm². The cells are grown attached at 37 °C in a humidified 5% CO_2 atmosphere, and provided with fresh medium every 2-3 day until proliferation in 75 cm² tissue culture flasks leads to excess of cells.

Fibroblast stock solution. In a typical experiment, the cells are grown until confluence of 80-90% is reached. The fibroblasts are then rinsed with 3 mL phosphate-buffered saline solution, and detached by incubating with 3 mL of trypsin-EDTA solution over 15 min. After addition of 8 mL of growth medium and manual cell count of a 0.5 ml aliquot with a hemocytometer and trypan blue solution, the cells are centrifuged at $125 \times g$ for 10 min. The pellet is re-suspended in complete growth medium to yield a cell suspension with a concentration of 1.1×10^5 cells/mL.

General assay procedure. In a typical assay, 190 μ L of the fibroblast suspension is incubated in 96-well plates with 10 μ L of antimicrobial agent at a nominal concentration of 1 \times 10⁵ cells/mL in humid 5% CO₂ atmosphere at 37 °C. After selected time intervals between 12 and 24 h, 20 μ L aliquots of resazurin dye are added, and the incubation continued for additional 4 h. For control experiments, 190 μ L of fibroblast and 10 μ L of antimicrobial agents are each separately incubated with medium. All experiments are conducted in octuplet.

Data collection and analysis. After incubation, fluorescence intensities are measured ($\lambda_{ex} = 535 \text{nm}$; $\lambda_{em} = 595 \text{nm}$) from the bottom of the plate as endpoint read with an integration time of 400 ms. The data are corrected for background effects and averaged. Cell viabilities are deduced from these data as a percent value by comparing the averaged intensity data for fibroblasts with and without antimicrobial agents.

ASSOCIATED CONTENT

Supporting Information. Details of the computational analysis of the dipole moment of **8a**; a Figure showing retained antimicrobial activity of selected microgels over 18 months. This material is available free of charge via the Internet at http://pubs.acs.org.

AUTHOR INFORMATION

Corresponding Author

* E-mail: <u>Susanne.Striegler@uark.edu</u>; phone: +1-479-575-5079; fax: -1-479-575-4049.

ORCID

Carlie M. Clem: 0000-0002-6600-0359 Babloo Sharma: 0000-0002-0265-322X Susanne Striegler: 0000-0002-2233-3784

Author Contributions

The manuscript was written through contributions of all authors. All authors have given approval to the final version of the manuscript. ‡C.C. and B.S. contributed equally to this work.

Notes

The authors declare no competing financial interests.

ACKNOWLEDGMENT

Support of this research to S.S. from the National Science Foundation (CHE-1854304) for the development of the microgels, and the Chancellor's Commercialization Fund at the University of Arkansas for development of antimicrobial assays,

ABBREVIATIONS

ATCC, Americal Type Culture Collection; CAPS, *N*-cyclohexyl-3-aminopropanesulfonic acid; DLS, dynamic light scattering; MBC, minimal bactericidal concentration; P, Polymer.

REFERENCES

- [1] Mulani, M. S.; Kamble, E. E.; Kumkar, S. N.; Tawre, M. S.; Pardesi, K. R., Emerging strategies to combat eskape pathogens in the era of antimicrobial resistance: A review, Frontiers in Microbiology 2019, 10, 1-24.
- [2] Li, S. Q.; Dong, S. J.; Xu, W. G.; Tu, S. C.; Yan, L. S.; Zhao, C. W.; Ding, J. X.; Chen, X. S., Antibacterial hydrogels, Advanced Science 2018, 5, 1-17.
- [3] Nystrom, L.; Al-Rammahi, N.; Haffner, S. M.; Stromstedt, A. A.; Browning, K. L.; Malmsten, M., Avidin-biotin cross-linked microgel multilayers as carriers for antimicrobial peptides, Biomacromolecules 2018, 19, 4691-4702.
- [4] Chen, M. H.; Xie, S. Z.; Wei, J. J.; Song, X. J.; Ding, Z. H.; Li, X. H., Antibacterial micelles with vancomycin-mediated targeting and ph/lipase-triggered release of antibiotics, ACS Applied Material Interfaces 2018, 10, 36814-36823.
- [5] Perreault, F.; de Faria, A. F.; Nejati, S.; Elimelech, M., Antimicrobial properties of graphene oxide nanosheets: Why size matters, ACS Nano 2015, 9, 7226-7236.
- [6] Sanchez-Lopez, E.; Gomes, D.; Esteruelas, G.; Bonilla, L.; Lopez-Machado, A. L.; Galindo, R.; Cano, A.; Espina, M.; Ettcheto, M.; Camins, A.; Silva, A. M.; Durazzo, A.; Santini, A.; Garcia, M. L.; Souto, E. B., Metal-based nanoparticles as antimicrobial agents: An overview, Nanomaterials 2020, 10, 39.
- [7] Preem, L.; Mahmoudzadeh, M.; Putrins, M.; Meos, A.; Laidmae, I.; Romann, T.; Aruvali, J.; Harmas, R.; Koivuniemi, A.; Bunker, A.; Tenson, T.; Kogermann, K., Interactions between chloramphenicol, carrier polymers, and bacteria-implications for designing electrospun drug delivery systems countering wound infection, Molecular Pharmaceutics 2017, 14, 4417-4430.
- [8] Kumar, P.; Takayesu, A.; Abbasi, U.; Kalathottukaren, M. T.; Abbina, S.; Kizhakkedathu, J. N.; Straus, S. K., Antimicrobial peptide-polymer conjugates with high activity: Influence of polymer molecular weight and peptide sequence on antimicrobial activity, proteolysis, and biocompatibility, ACS Appl. Mater. Interfaces 2017, 9, 37575-37586.
- [9] Malmsten, M., Antimicrobial peptides, Upsala Journal of Medical Sciences 2014, 119, 199-204.
- [10] Namivandi-Zangeneh, R.; Sadrearhami, Z.; Dutta, D.; Willcox, M.; Wong, E. H. H.; Boyer, C., Synergy between synthetic antimicrobial polymer and antibiotics: A promising platform to combat multidrug-resistant bacteria, ACS Infectious Diseases 2019, 5, 1357-1365.
- [11] Heimbuck, A. M.; Priddy-Arrington, T. R.; Padgett, M. L.; Llamas, C. B.; Barnett, H. H.; Bunnell, B. A.; Caldorera-Moore, M. E., Development of responsive chitosan-genipin hydrogels for the treatment of wounds, ACS Applied Bio Materials 2019, 2, 2879-2888.

- [12] Gupta, A.; Mumtaz, S.; Li, C. H.; Hussain, I.; Rotello, V. M., Combatting antibiotic-resistant bacteria using nanomaterials, Chemical Society Reviews 2019, 48, 415-427.
- [13] Frei, A.; Zuegg, J.; Elliott, A. G.; Baker, M.; Braese, S.; Brown, C.; Chen, F.; Dowson, C. G.; Dujardin, G.; Jung, N.; King, A. P.; Mansour, A. M.; Massi, M.; Moat, J.; Mohamed, H. A.; Renfrew, A. K.; Rutledge, P. J.; Sadler, P. J.; Todd, M. H.; Willans, C. E.; Wilson, J. J.; Cooper, M. A.; Blaskovich, M. A. T., Metal complexes as a promising source for new antibiotics, Chemical Science 2020, 11, 4531-4531.
- [14] Frei, A., Metal complexes, an untapped source of antibiotic potential?, Antibiotics 2020, 9, 90.
- [15] Regiel-Futyra, A.; Dąbrowski, J. M.; Mazuryk, O.; Śpiewak, K.; Kyzioł, A.; Pucelik, B.; Brindell, M.; Stochel, G., Bioinorganic antimicrobial strategies in the resistance era, Coordination Chemistry Reviews 2017, 351, 76-117.
- [16] Sierra, M. A.; Casarrubios, L.; de la Torre, M. C., Bioorganometallic derivatives of antibacterial drugs, Chemistry A European Journal 2019, 25, 7232-7242.
- [17] Biegański, P.; Szczupak, Ł.; Arruebo, M.; Kowalski, K., Brief survey on organometalated antibacterial drugs and metal-based materials with antibacterial activity, RSC Chemical Biology 2021, 2, 368-386.
- [18] Low, M. L.; Maigre, L.; Dorlet, P.; Guillot, R.; Pages, J. M.; Crouse, K. A.; Policar, C.; Delsuc, N., Conjugation of a new series of dithiocarbazate Schiff base copper(II) complexes with vectors selected to enhance antibacterial activity, Bioconjugate Chemistry 2014, 25, 2269-2284.
- [19] Kremer, E.; Facchin, G.; Estevez, E.; Albores, P.; Baran, E. J.; Ellena, J.; Torre, M. H., Copper complexes with heterocyclic sulfonamides: Synthesis, spectroscopic characterization, microbiological and sod-like activities: Crystal structure of Cu(sulfisoxazole)2(H2O)4 2H2O, Journal of Inorganic Biochemistry 2006, 100, 1167-1175.
- [20] Mondelli, M.; Brune, V.; Borthagaray, G.; Ellena, J.; Nascimento, O. R.; Leite, C. Q.; Batista, A. A.; Torre, M. H., New Ni(II)sulfonamide complexes: Synthesis, structural characterization and antibacterial properties. X-ray diffraction of Ni(sulfisoxazole)2(H2O)4 2H2O and Ni(sulfapyridine)2, Journal of Inorganic Biochemistry 2008, 102, 285-292.
- [21] Sharma, B.; Clem, C. M.; Perez, A. D.; Striegler, S., Antimicrobial activity of microgels with an immobilized copper(ii) complex linked to cross-linking and composition, ACS Applied Bio Materials 2020, 3, 7611-7619.
- [22] Striegler, S.; Dittel, M.; Kanso, R.; Alonso, N. A.; Duin, E. C., Hydrolysis of glycosides with microgel catalysts, Inorganic Chemistry 2011, 50, 8869-8878.
- [23] Striegler, S.; Pickens, J. B., Discrimination of chiral copper(ii) complexes upon binding of galactonoamidine ligands, Dalton Transaction 2016, 45, 15203-15210.
- [24] Sharma, B.; Striegler, S., Crosslinked microgels as platform for hydrolytic catalysts, Biomacromolecules 2018, 19, 1164–1174.
- [25] Antonietti, M.; Landfester, K., Polyreactions in miniemulsions, Progress in Polymer Science 2002, 27, 689-757.
- [26] Landfester, K.; Bechthold, N.; Tiarks, F.; Antonietti, M., Formulation and stability mechanisms of polymerizable miniemulsions, Macromolecules 1999, 32, 5222-5228.
- [27] Sharma, B.; Striegler, S.; Whaley, M., Modulating the catalytic performance of an immobilized catalyst with matrix effects a critical evaluation, ACS Catalysis 2018, 8, 7710-7718.
- [28] Sharma, B.; Pickens, J. B.; Striegler, S.; Barnett, J. D., Biomimetic glycoside hydrolysis by a microgel templated with a competitive glycosidase inhibitor, ACS Catalysis 2018, 8, 8788–8795.
- [29] Sharma, B.; Striegler, S., Tailored interactions of the secondary coordination sphere enhance the hydrolytic activity of cross-linked microgels, ACS Catalysis 2019, 9, 1686-1691.
- [30] Clinical and Laboratory Standards Institute (CLSI) Methods for dilution antimicrobial susceptibility tests for bacteria that grow aerobically In Approved Standard—Tenth Edition Clinical and Laboratory Standards Institute: Wayne, PA, 2015.

- [31] Kanso, R.; Striegler, S., Multi gram-scale synthesis of galactothionolactam and its transformation into a galactonoamidine, Carbohydrate Research 2011, 346, 897-904.
- [32] Arnold, F. H.; Striegler, S.; Sundaresan, V. Chiral ligand exchange adsorbents for amines and underivatized amino acids: 'Bait-and-switch' molecular imprinting, in Molecular and ionic recognition with imprinted polymers; American Chemical Society: 1998; Vol. 703, p 109-118.
- [33] Sharma, B.; Striegler, S., Nonionic surfactant blends to control the size and catalytic performance of microgels, ACS Catalysis 2020, 10, 9458–9463.
- [34] Gajda, T.; Jancsó, M. S.; Lönnberg, H.; Sirges, H., Crystal structure, solution properties and hydrolytic activity of an alkoxobridged dinuclear copper(ii) complex, as a ribonuclease model, Journal of the Chemical Society, Dalton Transaction 2002, 1757-1763.
- [35] McLellan, C.; Ngo, V.; Pasedis, S.; Dohlman, C. H., Testing the long term stability of vancomycin ophthalmic solution, International Journal of Pharmaceutical Compounding 2008, 12, 456-459
- [36] Galanti, L. M.; Hecq, J. D.; Vanbeckbergen, D.; Jamart, J., Long-term stability of vancomycin hydrochloride in intravenous infusions, Journal of Clinical Pharmacy and Therapeutics 1997, 22, 353–356
- [37] Mann, J. M.; Coleman, D. L.; Boylan, J. C., Stability of parenteral solutions of sodium cephalothin, cephaloridine, potassium penicillin g (buffered) and vancomycin hydrochloride, American Journal of Hospital Pharmacy 1971, 28, 760-763.
- [38] Malanovic, N.; Lohner, K., Antimicrobial peptides targeting gram-positive bacteria, Pharmaceuticals 2016, 9, 59.
- [39] Chen, C. Z.; Cooper, S. L., Interactions between dendrimer biocides and bacterial membranes, Biomaterials 2002, 23, 3359-3368.
- [40] Tan, M. C. S.; Carranza, M. S. S.; Linis, V. C.; Malabed, R. S.; Oyong, G. G., Antioxidant, cytotoxicity, and antiophidian potential of alstonia macrophylla bark, ACS Omega 2019, 4, 9488-9496.
- [41] Muniyandi, P.; Palaninathan, V.; Mizuki, T.; Maekawa, T.; Hanajiri, T.; Mohamed, M. S., Poly(lactic-co-glycolic acid)/polyethylenimine nanocarriers for direct genetic reprogramming of microrna targeting cardiac fibroblasts, ACS Applied Nano Materials 2020, 3, 2491-2505.
- [42] International Organization for Standardization Biological evaluation of medical devices part 5: Tests for in vitro cytotoxicity, In ISO 10993-5, International Organization for Standardization: Geneva, Switzerland, 2009.

